

A Cyclic CCK8 Analogue Selective for the Cholecystinin Type A Receptor: Design, Synthesis, NMR Structure and Binding Measurements

Stefania De Luca,^[a] Raffaele Ragone,^[b] Chiara Bracco,^[c] Giuseppe Digilio,^[c] Luigi Aloj,^[d] Diego Tesauro,^[a] Michele Saviano,^[a] Carlo Pedone,^[a] and Giancarlo Morelli*^[a]

A cyclic CCK8 analogue, cyclo^{29,34}[Dpr²⁹,Lys³⁴]-CCK8 (Dpr = L-2,3-diaminopropionic acid), has been designed on the basis of the NMR structure of the bimolecular complex between the N-terminal fragment of the CCK_A receptor and its natural ligand CCK8. The conformational features of cyclo^{29,34}[Dpr²⁹,Lys³⁴]-CCK8 have been determined by NMR spectroscopy in aqueous solution and in water containing DPC-d₃₈ micelles (DPC = dodecylphosphocholine). The structure of the cyclic peptide in aqueous solution is found to be in a relaxed conformation, with the backbone and Dpr29 side chain atoms making a planar ring and the N-terminal tripeptide extending approximately along the plane of this ring. In DPC/water, the cyclic peptide adopts a "boat-shaped" conformation, which is more compact than that found in aqueous solution. The cyclic constraint between the Dpr29 side chain and the CCK8 carboxyl terminus (Lys34) introduces a restriction in the backbone conformational freedom. However, the interaction of cyclo^{29,34}-

[Dpr²⁹,Lys³⁴]-CCK8 with the micelles still plays an important role in the stabilisation of the bioactive conformation. A careful comparison of the NMR structure of the cyclic peptide in a DPC micelle aqueous solution with the structure of the rationally designed model underlines that the turn-like conformation in the Trp30–Met31 region is preserved, such that the Trp30 and Met31 side chains can adopt the proper spatial orientation to interact with the CCK_A receptor. The binding properties of cyclo^{29,34}[Dpr²⁹,Lys³⁴]-CCK8 to the N-terminal receptor fragment have been investigated by fluorescence spectroscopy in a micellar environment. Estimates of the apparent dissociation constant, K_d , were in the range of 70–150 nM, with a mean value of 120 ± 27 nM. Preliminary nuclear medicine studies on cell lines transfected with the CCK_A receptor indicate that the sulfated-Tyr derivative of cyclo^{29,34}[Dpr²⁹,Lys³⁴]-CCK8 displaces the natural ligand with an IC_{50} value of 15 μ M.

Introduction

Cholecystinin (CCK) is a gut–brain peptide that exerts a variety of physiological actions in the gastrointestinal tract and central nervous system. The CCK peptide exists in different isoforms, which have different amounts of amino acids but are characterised by a conserved eight-residue sequence at the C terminal.^[1, 2] The biological action of CCK is mediated by two different membrane receptors, CCK_A (or CCK-1) and CCK_B (or CCK-2), that belong to the superfamily of G-protein-coupled receptors (GPCRs). These receptors are composed of seven transmembrane-spanning α -helical domains (TM) connected by alternating intracellular (IL) and extracellular loops (EL), with the N-terminus tail located on the extracellular side and the C-terminus tail on the cytoplasmic side. The CCK_A and CCK_B receptors are located predominantly in the gastrointestinal tract and the central nervous system, respectively.^[3] There is considerable interest in the pharmacology of the CCK_A and CCK_B receptors and, during the last few years, increasing effort has been put into developing selective CCK analogues endowed with agonist or antagonist activity.^[4, 5] Due to the fact that no high-resolution structure of any GPCR protein is available, all attempts to design CCK agonists and antagonists endowed with


enhanced selectivity towards the two receptors have been relying on the fact that most of the endogenous CCK peptides share the same C-terminal octapeptide (CCK26–33 or CCK8) and that modification of this octapeptide affects binding affinity and

[a] Prof. G. Morelli, Dr. S. De Luca, Dr. D. Tesauro, Dr. M. Saviano, Prof. C. Pedone
Centro Interuniversitario per la Ricerca sui Peptidi Bioattivi (CIRPeB)
& Istituto di Biostrutture e Bioimmagini del CNR
Via Mezzocannone, 6/8, 80134 Napoli (Italy)
Fax.: (+39) 81-5514305
E-mail: morelli@chemistry.unina.it

[b] Dr. R. Ragone
Dipartimento di Biochimica e Biofisica
Seconda Università di Napoli
Via Costantinopoli, 16, 80138 Napoli (Italy)

[c] Dr. C. Bracco, Dr. G. Digilio
Bioindustry Park del Canavese
Via Ribes, 5, 10010 Colletterto Giacosa (TO) (Italy)

[d] Dr. L. Aloj
Istituto di Biostrutture e Bioimmagini del CNR
Edificio 10, Via S. Pansini, 5, 80131 Napoli (Italy)

 Supporting information for this article is available on the WWW under <http://www.chembiochem.org> or from the author.

selectivity for receptor subtypes.^[1] On the basis of structure–activity relationships and conformational properties of this CCK8 fragment, several peptidic and nonpeptidic analogues have been proposed.^[4]

Recently, high-resolution structure information on the binding mode of CCK8 to the CCK_A and CCK_B receptors has appeared in the literature. This structural insight opens the way to a structure-based approach for the design of new CCK analogues. The NMR structure of the bimolecular complex between CCK8 and the N-terminal extracellular loop of the CCK_A receptor (fragment CCK_A-R(1–47)) has been solved by Pellegrini and Mierke.^[6] This study suggests that CCK8 binds to the CCK_A receptor with the C terminus of the ligand within the seven-helix bundle and the N terminus projecting out between transmembrane α -helices TM1 and TM7, thereby forming specific interactions with the N terminus of the CCK_A receptor. Successively, Giragossian and Mierke published^[7] the NMR structure of the complex formed by CCK8 with the third extracellular loop (EL3) of the CCK_B receptor, a structure that indicates a slightly different binding mode of CCK8 with the two receptor subtypes. An additional interaction between arginine residue 197 of the CCK_A receptor and the sulfate function present in [Tyr²⁷(SO₃H)]-CCK8 (the sulfated-Tyr form of CCK8) has been recently suggested.^[8, 9] This interaction should be responsible for the higher binding affinity and biological potency of the sulfated-Tyr form of CCK8 toward the CCK_A receptor, with respect to the nonsulfated peptide. Interestingly, the presence of the sulfate group does not affect the interaction between CCK8 and the CCK_B receptor. Thus, the sulfate function of [Tyr²⁷(SO₃H)]-CCK8 is useful for the efficient recognition and activation of the CCK_A receptor.

The structural information available allowed us to design the CCK8 analogue cyclo^{29,34}[Dpr²⁹,Lys³⁴]-CCK8 (compound 1, Scheme 1), whose bioactive conformation is expected to be stabilised by a cyclic skeleton. To the best of our knowledge, this is the first attempt to design a peptidic CCK analogue on the basis of the structure of the bimolecular complex between the

CCK_A receptor and its natural ligand. The solution structure of 1 has been worked out by NMR techniques and compared to the structure adopted by CCK8 in the complex with the receptor fragment CCK_A-R(1–47), while the binding properties of 1 to the receptor fragment have been investigated by fluorescence spectroscopy in a micellar environment. The binding properties of the sulfated-Tyr derivative of 1 (compound 2, Scheme 1) have been tested by preliminary nuclear medicine studies on cell lines transfected with the CCK_A receptor.

Results and Discussion

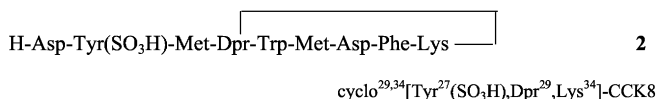
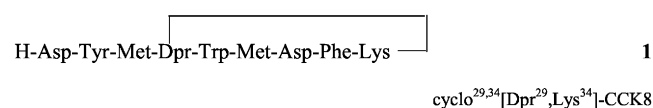
Peptide design

The starting point for the rational design of a CCK8 peptidomimetic agonist is the bimolecular complex between CCK8 and fragment 1–47 of the CCK_A receptor (CCK_A-R(1–47), corresponding to the N-terminal extracellular arm plus a few residues belonging to the first TM1 helix). The structure of this complex has been obtained by Pellegrini and Mierke by NMR spectroscopy and molecular dynamics simulations in dodecylphosphocholine (DPC) micelles (PDB code: 1D6G).^[6] The elucidation of the ligand–receptor complex was built upon the detection of intermolecular NOE interactions between Tyr27 and Met28 of CCK8 and W39 of CCK_A-R(1–47). (Three letter amino acid codes denote residues in the peptide ligand and single letter codes denote receptor residues throughout the text.) The complex is stabilised by a number of hydrophobic, coulombic and hydrogen-bonding interactions. The hydrophobic interactions are due to the close proximity between the side chains of Tyr27 and P35/W39, Met28 and W39/A42 and, finally, Met32 and L46. The complex is further stabilised by the coulombic interactions between Asp26 of the ligand and K37, E38, and Q40 of CCK_A-R(1–47). Finally, hydrogen-bonding interactions are detected involving the Met32 NH and Met32 CO moieties of CCK8 with the Q43 CO ϵ and Q43 NH ϵ moieties of the receptor, respectively. Analysis of the bimolecular complex underlines that the contact region in the complex involves residues P33, P35–Q40, A42, Q43, L46 and L47 of the receptor and segment Tyr27–Met31 of the ligand. As far as the conformations of CCK8 and CCK_A-R(1–47) are concerned, it is worth noting that NMR data together with extensive molecular dynamics simulations indicate that the structures of the two separate molecules do not undergo major conformational changes upon complex formation. CCK8 adopts a conformation that is stabilised by a weak intramolecular 4 \rightarrow 1 hydrogen bond between the Gly29 CO and Asp32 NH moieties, with the formation of a β -turn-like structure.

The rational design of the CCK8 analogue has been done according to the following considerations: 1) the conformational features of the segment encompassing residues Tyr27–Met31, which are critical for high-affinity receptor binding, should be conserved, 2) the backbone flexibility of the new analogue should be minimised to stabilise the bioactive conformation and 3) resistance to enzymatic degradation should be enhanced. To match all these requirements we have introduced a cyclic constraint into the covalent structure. Gly29 in CCK8 has been replaced with an L-2,3-diaminopropionic acid (Dpr) residue to

H-Asp²⁶-Tyr²⁷-Met²⁸-Gly²⁹-Trp³⁰-Met³¹-Asp³²-Phe³³-amide

CCK8



Scheme 1. Amino acid sequence of CCK8 and of the cyclic analogue in its free (1) and sulfated (2) forms. The adopted numbering scheme of 26–33 follows that of full-length CCK (a 33-residue-long peptide, with CCK8 being the C-terminal octapeptide segment). The endogenous CCK8 peptide is amidated on the C-terminal end.

provide a side-chain amino group able to make a cyclic structure through an amide bond. To introduce a cyclic constraint between the Dpr29 side chain and the CCK8 carboxyl terminus (Phe33) without modifying the CCK8 bioactive conformation, one more residue had to be added to the C-terminal end of the peptide. An L-lysine residue (Lys34) has been added to the carboxyl terminus of Phe33 and then the lysine carboxyl terminus has been linked to the γ -amino group of the Dpr29 side chain. The choice of L-Lys was dictated by the possible use of the lysine $N\epsilon$ amino group to introduce further chemical functionalities. (Conjugation to a chelating agent to obtain a metal-labelled derivative is currently under development.) The covalent structure of the rationally designed CCK8 analogue cyclo^{29,34}[Dpr²⁹,Lys³⁴]-CCK8 (**1**) is depicted in Scheme 1.

To check whether the conformation of cyclo^{29,34}[Dpr²⁹,Lys³⁴]-CCK8 was effectively endowed with the structural requirements for high-affinity binding, a model of the bimolecular complex between cyclo^{29,34}[Dpr²⁹,Lys³⁴]-CCK8 and CCK_A-R(1–47) has been built by analogy to the complex of CCK8/CCK_A-R(1–47). This model was energy minimised to refine the complex structure (Figure 1) by following a two-step procedure. Firstly, the cyclo^{29,34}[Dpr²⁹,Lys³⁴]-CCK8 compound was minimised to eliminate any "hot spots" introduced in the design stage. During this step all receptor residues were kept fixed at their original positions. Then, the restraints were removed and a further energy minimisation was performed. The minimised model keeps all the desired key interactions. The energy-minimised cyclo^{29,34}[Dpr²⁹,Lys³⁴]-CCK8 structure has been superimposed onto the CCK8 experimental structure to show the degree of similarity between the designed and template molecules (Figure 2). The analysis of the conformation of each residue in both peptides shows that only Phe33 in cyclo^{29,34}[Dpr²⁹,Lys³⁴]-CCK8 presents a large deviation from the conformation assumed in CCK8. This distortion is partially due to the cyclic constraint introduced into the molecule and is not expected to interfere with receptor binding.

Peptide synthesis

The linear precursors of the cyclic compounds **1** and **2** were synthesised by the solid-phase method with standard 9-fluorenylmethoxycarbonyl (Fmoc) chemistry. The tyrosine derivative Fmoc-Tyr(SO₃H) barium salt was used in the case of peptide **2**. For both peptide syntheses the orthogonally protected Fmoc-Dpr(Dde)-OH residue was used (Dde = 1-(4,4-dimethyl-2,6-dioxo-cyclohexylidene)-3-methylbut-

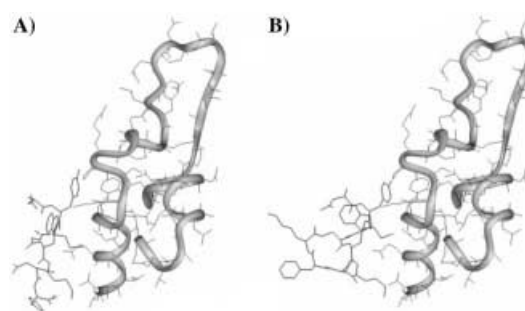


Figure 1. Molecular models of a) the CCK8/CCK_A-R(1–47) complex (ref. [6]; PDB code: 1D6G) and b) the theoretical Cyclo^{29,34}[Dpr²⁹,Lys³⁴]-CCK8/CCK_A-R(1–47). The CCK_A-R(1–47) section is represented with a ribbon.

yl). The superacid-labile 2-chlorotriptyl chloride resin was used in order to obtain the whole peptides completely protected upon cleavage from the resin. In both cases the Dpr β -NH₂ groups were deprotected from Dde before cleavage. This procedure allowed us to obtain peptides with the Dpr β -NH₂ and C-terminal carboxyl groups free from protecting groups and ready for N–C cyclisation. Cyclisation was performed in CH₂Cl₂ by using benzotriazole-1-yloxy-trispyrrolidinophosphonium (PyBOP) as the carboxyl group activant and *N,N*-diisopropylethylamine (DIPEA) as the base. The cyclic peptide **1** was completely deprotected on the amino acid side chains by using standard procedures and was purified by HPLC. The final yield of product **1** was 20%. To minimise the loss of sulfate groups during the

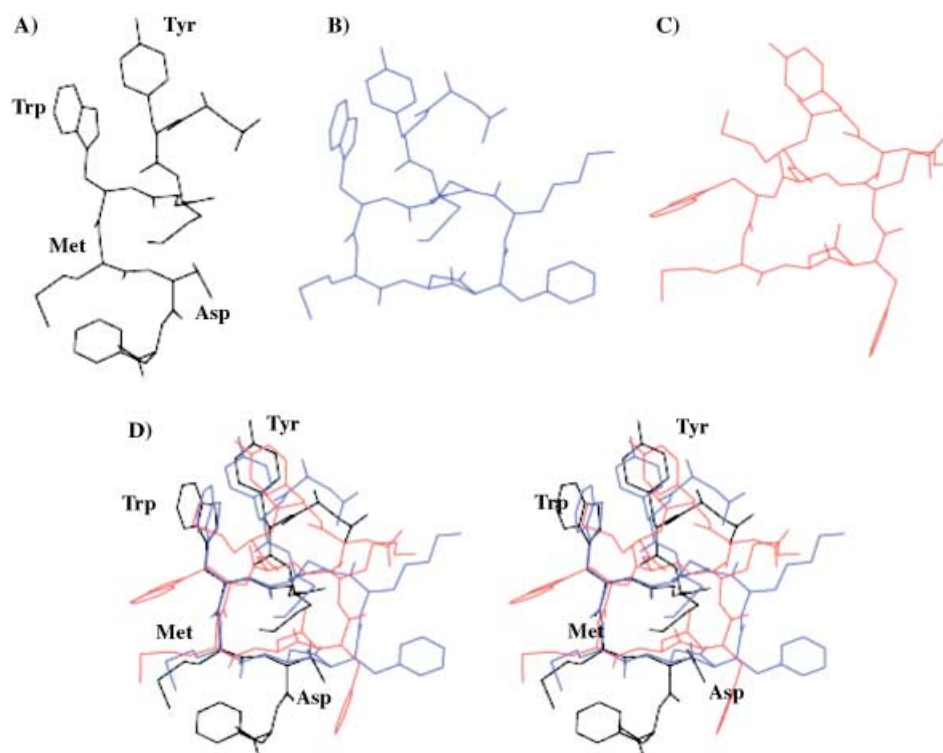


Figure 2. Structures of: A) CCK8 in the CCK8/CCK_A-R(1–47) complex (ref. [6]; PDB code: 1D6G), B) cyclo^{29,34}[Dpr²⁹,Lys³⁴]-CCK8 (energy-minimised theoretical model), C) cyclo^{29,34}[Dpr²⁹,Lys³⁴]-CCK8 (NMR structure in DPC/water solution). D) Stereoview of the structures shown in (A), (B) and (C) in the same orientation after the best superposition.

final deprotection of peptide **2**, the protected cyclic peptide was treated with a mixture of $\text{CF}_3\text{COOH}/\text{H}_2\text{O}/2\text{-methylindole}/m\text{-cresole}$ (87:10:2:1) for 16 hours at $+4^\circ\text{C}$.^[10] No significant loss of sulfate was observed and after HPLC purification the yield was 13%. The purity and identity of the resulting peptides were confirmed by analytical reversed-phase HPLC (RP-HPLC) and MALDI-TOF mass spectrometry.

^1H NMR studies

The ^1H NMR structure of $\text{cyclo}^{29,34}[\text{Dpr}^{29},\text{Lys}^{34}]\text{-CCK8}$ (**1**) has been solved both in aqueous solution and in water containing DPC- d_{38} micelles.

Aqueous solution: The NMR spectra of $\text{cyclo}^{29,34}[\text{Dpr}^{29},\text{Lys}^{34}]\text{-CCK8}$ in aqueous solution at pH 6.4 are characterised by sharp resonances within the temperature range 285–310 K, apart from that of the Tyr27 HN moiety which is broadened because of chemical exchange. An expansion of the aromatic/amide region of the ^1H NMR spectrum of $\text{cyclo}^{29,34}[\text{Dpr}^{29},\text{Lys}^{34}]\text{-CCK8}$ (1.4 mM, $\text{H}_2\text{O}/\text{D}_2\text{O}$ 94%, pH 6.4, $T=285$ K) with resonance assignment is shown in Figure 3 (top trace), while chemical shifts are listed in Table 1. Sequential assignment revealed a single resonance for each proton, a fact indicating that conformational averaging processes (if any) must be fast on the chemical shift timescale. Despite the small size of the peptide, NOESY spectra (mixing time: 300–450 ms) showed cross-peaks having the same sign as diagonal peaks, which

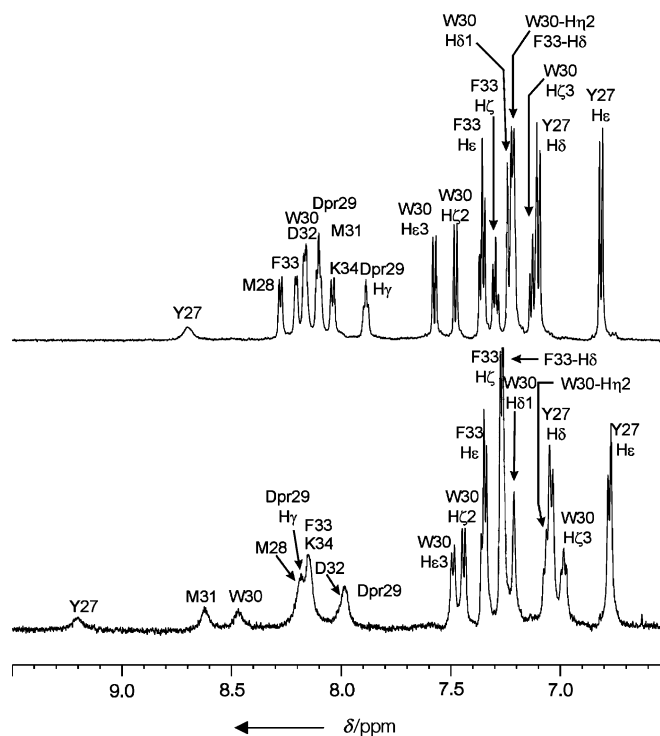


Figure 3. Expansion of the aromatic/amide regions of the ^1H NMR spectra of $\text{cyclo}^{29,34}[\text{Dpr}^{29},\text{Lys}^{34}]\text{-CCK8}$ (1.4 mM, $\text{H}_2\text{O}/\text{D}_2\text{O}$ 94%, pH 6.4, $T=285$ K) in aqueous solution (top) and in the presence of 174 mM DPC- d_{38} (bottom), with resonance assignments.

Table 1. ^1H NMR chemical shifts of $\text{cyclo}^{29,34}[\text{Dpr}^{29},\text{Lys}^{34}]\text{-CCK8}$ in aqueous solution and DPC/water solution at 285 K.^[a]

Residue	^1H atom	Chemical shift in:	
		water ^[b]	DPC/water ^[c]
Asp26	H α	4.14	4.23
	others	2.77/2.66 (H β)	2.81/2.73 (H β)
Tyr27	HN	8.69	9.2
	H α	4.53	4.11
Met28	others	2.99 (H β), 7.11 (H δ), 6.81 (H ϵ)	2.94/2.86 (H β), 7.04 (H δ), 6.78 (H ϵ)
	HN	8.28	8.18
	H α	4.31	4.21
Dpr29	others	1.82 (H β), 2.35/2.30 (H γ), 1.94 (H ϵ)	1.69 (H β), 2.32/2.20 (H γ), 1.97 (H ϵ)
	HN	8.11	7.99
	H α	4.39	4.46
Trp30	others	3.56 (H β), 7.89 (H γ)	3.77/3.43 (H β), 8.19 (H γ)
	NH	8.17	8.47
	H α	4.66	4.60
Met31	others	3.26 (H β), 7.25 (H δ 1), 7.58 (H ϵ 3), 10.22 (H ϵ 1), 7.13 (H ζ 3), 7.48 (H ζ 2), 7.21 (H η 2)	3.24 (H β), 7.22 (H δ 1), 7.49 (H ϵ 3), 10.60 (H ϵ 1), 6.98 (H ζ 3), 7.44 (H ζ 2), 7.06 (H η 2)
	NH	8.10	8.62
	H α	4.17	4.26
Asp32	others	1.82/1.68 (H β), 1.99/1.91 (H γ), 2.00 (H ϵ)	2.05/1.95 (H β), 2.44/2.31 (H γ), 2.06 (H ϵ)
	NH	8.17	8.00
	H α	4.29	4.46
Phe33	others	2.62/2.65 (H β)	2.80/2.64 (H β)
	NH	8.21	8.15
	H α	4.36	4.33
Lys34	others	3.22/3.19 (H β), 7.22 (H δ 1), 7.36 (H ϵ 1), 7.30 (H ζ)	3.27/3.24 (H β), 7.27 (H δ 1), 7.35 (H ϵ 1), 7.34 (H ζ)
	NH	8.04	8.15
	H α	4.22	4.29
	others	1.81/1.66 (H β), 1.15 (H γ), 1.58 (H δ), 2.93 (H ϵ)	1.80/1.68 (H β), 1.23 (H γ), 1.62 (H δ), 2.94 (H ϵ)

[a] The assignment of diastereotopic atom pairs is not stereospecific. [b] Conditions: 1.4 mM $\text{cyclo}^{29,34}[\text{Dpr}^{29},\text{Lys}^{34}]\text{-CCK8}$, $\text{H}_2\text{O}/\text{D}_2\text{O}$ 90%, pH 6.4, $T=285$ K. [c] Conditions: 1.4 mM $\text{cyclo}^{29,34}[\text{Dpr}^{29},\text{Lys}^{34}]\text{-CCK8}$, 174 mM DPC- d_{38} , $\text{H}_2\text{O}/\text{D}_2\text{O}$ 90%, pH 6.4, $T=285$ K.

indicates that the correlation time for molecular motions falls in the slow motion regime (negative NOE). To gain more insights into the structural features of cyclo^{29,34}[Dpr²⁹,Lys³⁴]-CCK8 a conformation analysis of the compound has been performed based on geometric constraints derived from NOE measurements. The NOESY spectrum acquired at 285 K with a mixing time of 450 ms was used to derive the geometric constraints, as these conditions represented the best compromise between sensitivity and minimisation of artefacts due to spin diffusion. The analysis of this NOESY spectrum allowed for the derivation of a total of 75 meaningful geometric constraints to be used in structure optimisation (see Table 2). Only two nonsequential NOE interactions were found (Tyr27 H ϵ /Dpr29 H α and Asp32 H β /Lys34 HN), apart from those NOE interactions involving residues that are adjacent because of the cyclo moiety (NOE interactions between residues Dpr29 and Lys34). The absence of relevant constraints other than intrasidue or sequential ones may be due to the combination of both conformational flexibility and unfavourable molecular size. However, the fact that a ROESY experiment (mixing time: 350 ms) provided no correlations other than those found in the NOESY spectra suggests that flexibility is the major cause for the low number and intensity of the NOE signals. In analogy to *cis* peptide bonds, the absence of NOE interactions between the Lys34 H α and Dpr29 H β protons suggests a *trans* geometry of the amide bond closing the cyclic moiety between Dpr29 and Lys34. The *trans* geometry of this bond has been confirmed as follows. Initially, 40 random conformers of **1** were built with *trans* geometries at the

Dpr29/Lys34 amide bond and subjected to unconstrained molecular dynamics simulations and energy minimisation. This operation was repeated for another set of 40 conformers on which a *cis* geometry was imposed. The analysis of the *trans* structures revealed characteristically short average distances between the Dpr29 H γ and Lys34 HN protons (average 2.6, min 1.7, max 3.8 Å) and between the Dpr29 H γ and Lys34 H α protons (average 2.9, min 2.2, max 3.6 Å). On the other hand, the corresponding distances in the *cis* structures were found to be significantly longer (by 1 Å or more). As the upper limit distances obtained by the NOE measurements are very close to those expected for a *trans* geometry (3.0 Å for Dpr29 H γ /Lys34 HN, 3.5 Å for Dpr29 H γ /Lys34 H α), it is concluded that in aqueous solution **1** adopts a *trans* geometry, in agreement with the known higher stability of *trans* geometries. Thus, all subsequent calculations have been performed by keeping the *trans* geometry fixed. The solution structure of **1** has been obtained by generating 800 conformers of **1** and optimizing each of them by constrained TAD and simulated annealing. A subgroup of 30 conformers showing the lowest target functions was then selected out of the bundle of acceptable optimised conformers for further energy minimisation and structure analysis. This subgroup of structures showed a good nonbonded geometry and good consistency with the NOE-derived constraints, as testified by 1) the low target function values (average 0.06 Å²), 2) the absence of significant violations of van der Waals constraints and 3) the absence of violations larger than 0.2 Å for the NOE-derived upper limit distances. These structures were

refined further by 50-ps constrained molecular dynamics at a temperature of 300 K followed by energy minimisation. The refinement step was carried out in vacuo with the AMBER force field, which allows for a more detailed treatment of the energetic terms due to nonbonded interactions. A superposition of 15 optimised structures where the root mean square deviation (RMSD) between the heavy atoms of the cyclic backbone (residues 29–34) have been minimised is shown in Figure 4. The RMSD between the backbone atoms of residues 27–34 was 1.28 Å, whereas it decreased to 0.67 Å when calculated over the cyclic part of the peptide (residues 29–34). The analysis for the short-range order (RMSDs calculated over the superposition of three-residue segments) indicated that the structures showed a relatively good definition of the backbone conformation within the cyclic moi-

Table 2. Summary of the NMR-derived constraints used for torsion angle dynamics (TAD) with simulated annealing calculations and results from structure optimisation of cyclo^{29,34}[Dpr²⁹,Lys³⁴]-CCK8.

	Water <i>T</i> = 285 K ^[a]	DPC/water <i>T</i> = 300 K ^[b]
Interproton upper distance bounds from NOEs:		
total number	75	89
intrasidue	42	50
<i>i, i + 1</i>	25	36
<i>i, i + 2</i>	2	3
<i>i, i + 3</i>	0	0
<i>i, i + 4</i>	0	0
<i>i, i + 5</i> ^[c]	6	0
Structure calculation: ^[d]		
residual target function \pm SD ^[e] [Å ²]	0.057 \pm 0.008	0.055 \pm 0.009
violations of upper distance bounds: ^[f]		
> 0.2 Å	0	0
> 0.1 Å	2	1
violations of Van der Waals lower bounds: ^[f]		
> 0.1 Å	0	0
global RMSD \pm SD ^[e] [Å]: ^[d]		
segment 27–34 (backbone)	1.28 \pm 0.41	0.97 \pm 0.37
segment 27–34 (heavy atoms)	3.00 \pm 0.74	2.62 \pm 0.70
segment 29–34 (backbone)	0.67 \pm 0.29	0.31 \pm 0.15
segment 29–34 (heavy atoms)	2.19 \pm 0.65	1.36 \pm 0.31
segment 29–31 (backbone)	0.31 \pm 0.13	0.08 \pm 0.04
segment 29–31 (heavy atoms)	1.55 \pm 0.72	0.65 \pm 0.23
[a] Conditions: 1.4 mM cyclo ^{29,34} [Dpr ²⁹ ,Lys ³⁴]-CCK8, H ₂ O/D ₂ O 94%, pH 6.4, NOESY mixing time of 450 ms.		
[b] Conditions: 1.4 mM cyclo ^{29,34} [Dpr ²⁹ ,Lys ³⁴]-CCK8, 174 mM DPC- <i>d</i> ₅₆ , H ₂ O/D ₂ O 94%, pH 6.4, NOESY mixing time of 150 ms. [c] All of them are between Dpr29 and Lys34. [d] Statistics calculated over an group of thirty structures endowed with a minimal residual target function. [e] SD = standard deviation. [f] Violations consistently found in at least one-third of the analysed structures.		

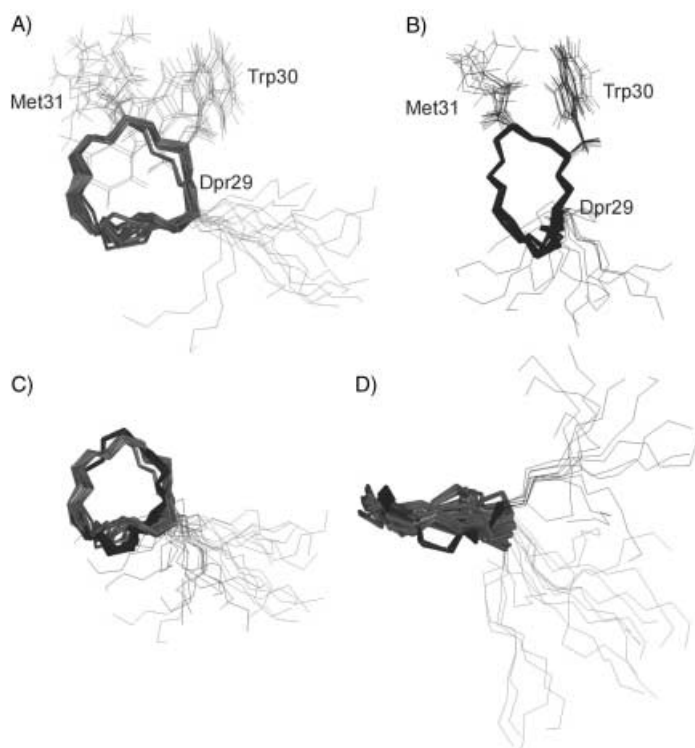


Figure 4. NMR structures of cyclo^{29,34}[Dpr²⁹,Lys³⁴]-CCK8 obtained by means of torsion angle dynamics (TAD) with simulated annealing, restrained molecular dynamics and energy minimisation. A), B) Superposition of 15 structures obtained in aqueous solution (A) and in DPC/water (B). The RMSD between heavy atoms belonging to the cyclic part of the molecule (backbone atoms of segment 29–34 and side-chain atoms of Dpr29, thicker lines) has been minimised. In A) and B) the side chains of Trp30 and Met31 are also shown. C), D) Comparison between the structures of cyclo^{29,34}[Dpr²⁹,Lys³⁴]-CCK8 in aqueous solution (15 structures, grey) and those in DPC/water (15 structures, black). Two different views are given. The backbone and the Dpr29–Lys34 bridge are shown with thicker lines. All 30 structures were superposed to minimise the RMSD between heavy atoms belonging to the cyclic part of the molecule (backbone atoms of segment 29–34 and side-chain atoms of Dpr29).

ety (Figure 5), even though no regular secondary structure motifs could be clearly identified. An ill-defined turn-like structure may be envisaged to encompass residues 31–34, as characteristic Phe33 HN/Lys34 HN, Phe33 H α –H β /Lys34 HN and Asp32 H α –H β /Phe33 HN NOE interactions have been found, together with a Lys34 ³J_{HN-H α value of 4.8 Hz. However, the rather high temperature coefficient of the Lys34 HN proton, the relatively long Phe33 HN/Lys34 HN distance and the fact that only 40% of the refined structures show a hydrogen bond between the Lys34 HN and Met31 CO moieties indicates that this turn is distorted and is probably subjected to conformational averaging.}

DPC micelles: On going from an aqueous to a DPC micelle solution (174 mM DPC-*d*₃₈), a general increase in the line width of the proton resonances and a remarkable change in the chemical shift values of a large number of resonances are observed, facts indicating that the peptide interacts with the micelles (Figure 3). This interaction is quite strong, as indicated by the severe line broadening observed when 3.2 mM 5-doxylstearate (5-DS) is added to the micelles (see below). Although the line width

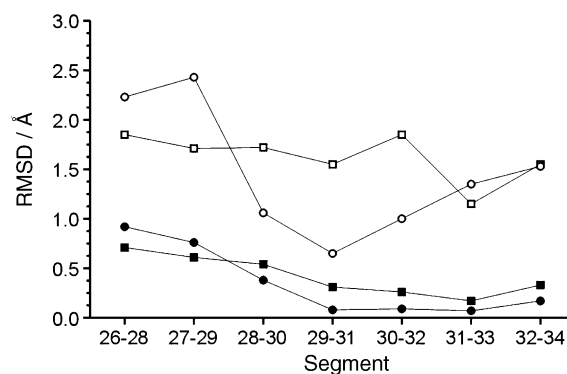


Figure 5. Plot of the atomic backbone RMSDs (solid symbols: backbone heavy atoms; open symbols: all heavy atoms) calculated over the superposition of consecutive three-residue segments against the position of the segment in the amino acid sequence. Squares: in water, circles: in DPC/water. The RMSDs were calculated over superposition of thirty structures.

increased, it was still possible to assign almost all of the resonances. As in the case of the aqueous solution, no appreciable changes in the line widths and a single signal for each proton were observed within the temperature range 285–310 K. To assess whether the micelles could stabilise a preferential conformation, the structure of the compound has been worked out on the basis of geometric constraints obtained from a NOESY spectrum acquired with a mixing time of 150 ms ($T = 300$ K). Line broadening and signal overlap actually made the assignment or integration of a number of NOE peaks somewhat ambiguous. Unfortunately, spectral overlap between the Dpr29 H γ and Lys34 HN signals hampered the direct assessment of the conformation around the Dpr29/Lys34 amide bond. A *trans* geometry was assumed on the basis of the absence of NOE interactions between the Lys34 H α and Dpr29 H β protons. Ambiguously assigned peaks, including those involving the Dpr29 H γ and Lys34 HN protons, were not considered for structure optimisation. Nevertheless, a total of 89 meaningful constraints were obtained from NOE measurements, a number significantly bigger than that found in aqueous solution (Table 2). This indicates that 1) the peptide structure is made more rigid by the interaction with the micelles and/or 2) the interaction with the micelles definitively pushes the correlation times for molecular motions into the slow motion regime, thus increasing the sensitivity of the NOE measurements. However the low number of nonsequential or nonintraresidue NOE interactions indicates the absence of well-defined regular secondary structure motifs. Structure optimisation was executed by following essentially the same protocol as that used to obtain the structure in water. The calculations converged to a group of structures that were highly consistent with the input constraints and were also characterised by good steric consistency (the average target function was 0.055 Å², calculated over a subgroup comprising the best 30 structures). A superposition of 15 optimised structures, where the RMSD between the heavy atoms of the cyclic backbone (residues 29–34) has been minimised, is shown in Figure 4. The RMSD between the backbone atoms of residues 27–34 was 2.42 Å, whereas it

decreased to 0.31 Å when calculated over the cyclic part of the peptide (residues 29–34). The structure of cyclo^{29,34}[Dpr²⁹,Lys³⁴]-CCK8 in DPC/water appears to be more well defined than that obtained in aqueous solution, as is clear from the comparison of the backbone and the all-heavy-atoms RMSDs calculated over three-residue segments (Table 2, Figure 5). Remarkably, a minimum in the RMSD (all heavy atoms) is observed in segment 29–34, thereby indicating a higher degree of conformational order not only in the cyclic moiety (the side chain of Dpr29 closes the ring) but also in the conformation of the side chains of Trp30 and Met31. This conformational order may be induced by the interaction with the micelle. To assess whether a given residue has a preferential role in interacting with the micelle surface, 5-DS was added to the cyclo^{29,34}[Dpr²⁹,Lys³⁴]-CCK8/DPC micelle system. Under our experimental conditions ([DPC] = 174 mM, [5-DS] = 3.2 mM), 5-DS has been shown to completely insert within DPC micelles without causing an appreciable modification of their structure, with each micelle containing no more than one molecule of spin label.^[11] Upon addition of 5-DS, a broadening of the peptide resonances is generally observed, which confirms the strong interaction between the peptide and the micelle. Measurements of T_1 relaxation times for the signals in the amide/aromatic region showed that the signals of the Trp30 indole ring were most affected by the addition of 5-DS. This finding supports the view that the Trp30 side chain makes contacts with the membrane and provides an explanation for the restriction of conformational freedom of the Trp30 side chain.

Further evidence about the structure-promoting role of the peptide/micelle interaction can be obtained by analysis of the amide proton chemical shift temperature coefficients $\Delta\delta/\Delta T$ (Figure 6). In the aqueous solution, these coefficients are always negative (chemical shifts decrease as the temperature increase) and show relatively modest variations along the amino acid sequence ($\Delta\delta/\Delta T$ values fall between -5.9 and -2.9 ppbK⁻¹).

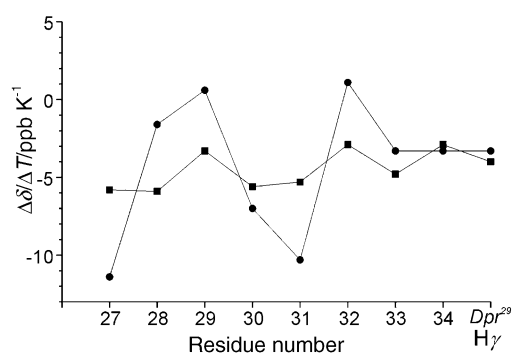


Figure 6. Temperature coefficients of the amide protons ($\Delta\delta/\Delta T$ in ppbK⁻¹) of cyclo^{29,34}[Dpr²⁹,Lys³⁴]-CCK8 against the position of the residue in the amino acid sequence. Squares: in water, circles: in DPC/water.

This finding indicates that $\Delta\delta/\Delta T$ coefficients are essentially dominated by the rate of chemical exchange between the amide protons and the solvent and that the molecule is rather flexible. In the presence of DPC micelles, the spreading of the $\Delta\delta/\Delta T$ values between different amide protons significantly increases, with the amide protons of Dpr29 and Asp32 having slightly

positive values and those of Tyr27 and Met31 having very large negative values. In this case, the temperature coefficients do not show a clear correlation with hydrogen bonding or solvent protection as far as can be guessed from the NMR structure. For instance, calculation of hydrogen bonds or solvent accessibility for each of the amide protons belonging to the cyclic moiety (segment 29–34) indicate that such protons are uniformly shielded from solvent; nevertheless, they show a large variability in their temperature coefficient. Moreover, the Met28 HN proton shows a very small $\Delta\delta/\Delta T$ value, despite the fact that it is not involved in any significant hydrogen-bonding interactions. Thus, the shielding of the amide protons from solvent exchange must be essentially dominated by the interaction between the peptide and the micelle, rather than by intramolecular interactions. The fact that $\Delta\delta/\Delta T$ coefficients in the DPC micelle solution show larger variations than in aqueous solution indicates that the interaction with the micelle leads to a larger differentiation of the chemical environment around each of the amide protons and, hence, to a structure that is more rigid than in aqueous solution.

In summary, the cyclic moiety in aqueous solution adopts a relaxed conformation, with the backbone and Dpr29 side-chain atoms making a planar ring and the first three N-terminal residues extending approximately along the plane of the ring (Figure 4). In DPC/water, the cyclic moiety adopts a “boat-shaped” conformation, that is more compact than that found in aqueous solution. The three-residue N-terminal tail extends outside the plane of the ring, even though the exact conformation of the N-terminal dipeptide segment could not be uniquely defined because of the lack of significant NOE interactions. Although the cyclic constraint between the Dpr29 side chain and the CCK8 carboxyl terminus (Lys34) introduces a restriction of backbone conformational freedom, the interaction with the micelles still appears to play an important role in the stabilisation of the bioactive conformation, at least within the region encompassing residues Trp30 and Met31. Comparison of the NMR structure in DPC/water with that of the designed model (Figure 2) underlines that, within the cyclic moiety, the turn-like conformation in the Trp30–Met31 and Phe33–Lys34 regions is preserved. (The backbone heavy-atom RMSD calculated from the best superposition of the cyclic moiety has a value of 0.78 Å.) This important feature, observed in the DPC/water environment, brings the side chains of Trp30 and Met31 into the proper spatial orientation to interact with the CCK_A receptor. The fact that the cyclic analogue maintains the correct conformation is further supported by a comparison between the NMR structures of cyclo^{29,34}[Dpr²⁹,Lys³⁴]-CCK8 and CCK8^[6] (Figure 2). The RMSD after the best superposition of backbone heavy atoms within segment Trp30–Asp32 is 0.45 Å.

Fluorescence spectroscopy

The excitation wavelength used for fluorescence titrations was the same as that previously adopted to monitor the binding of nonsulfated CCK8 to CCK_A-R(1–47)^[12] because cyclo^{29,34}-[Dpr²⁹,Lys³⁴]-CCK8 contains the same fluorophores as those contained in CCK8 (one Phe, one Tyr and one Trp residue). Thus,

considering that the Phe and Tyr chromophores absorb negligibly at wavelengths higher than 270 and 290 nm, respectively, fluorescence was excited at 295 nm, where it can be assumed that emission spectra originate only from the Trp residue. Experiments were performed in the presence of sodium dodecylsulfate (SDS) at a concentration of 6–8 mM, which is close to the critical micellar concentration of SDS in pure water as measured by fluorescence spectroscopy.^[13, 14] At the ionic strength of the titration experiments, it was found that the micellar aggregation of SDS, occurring at ≈ 5 mM, overlapped with secondary and tertiary structural rearrangements of CCK_A-R(1–47). It was then inferred that the detergent binds to CCK_A-R(1–47) in micellar form, thus mimicking a membrane-like environment.^[12] Figure 7 shows a typical saturation experiment, performed under the conditions described above. Unlike CCK8,^[12] the fluorescence signal increased, but modifications

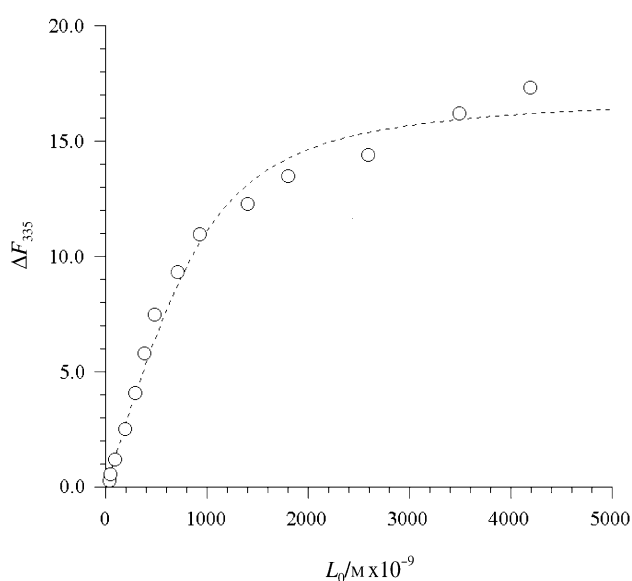


Figure 7. Binding of cyclo^{29,34}[Dpr²⁹,Lys³⁴]-CCK8 to CCK_A-R(1–47). The concentration of the receptor fragment was 0.98 μ M (in 10 mM phosphate buffer (pH 7.2) with 6 mM SDS). Fluorescence intensities at 335 nm were smoothed as described in the text. The binding curve was generated by using the mean value of K_d (120 nM), as estimated from Equation (2).

originating from binding were still small in comparison to the separate contributions of cyclo^{29,34}[Dpr²⁹,Lys³⁴]-CCK8 and CCK_A-R(1–47). In any case, binding curves from several experiments, obtained with receptor concentrations of 0.49–2.40 μ M, were independent of the emission wavelength chosen to perform the calculations. Estimates of the apparent dissociation constant, K_d , were in the range of 70–150 nM with a mean value of 120 ± 27 nM, which is about half of the K_d value for CCK8 binding to CCK_A-R(1–47).^[12]

The range of affinities found for the binding of several linear CCK8 analogues to B-type pancreatic receptors is submicromolar^[15] and thus compares well with our values for the binding of linear nonsulfated CCK8^[12] and cyclo^{29,34}[Dpr²⁹,Lys³⁴]-CCK8 to CCK_A-R(1–47). However, the affinities of C-terminal-sulfated CCK8 toward CCK_A and CCK_B receptors are nanomolar^[16] and

the interaction of both sulfated and nonsulfated cyclic CCK8 analogues with B-type binding sites is characterised by subnanomolar dissociation constants.^[15] It seems reasonable that these differences are, to a large extent, attributable to the structure of the CCK_A-R(1–47) fragment, which however is a reliable model system to monitor the ability of the newly synthesised CCK analogue to bind the cholecystokinin receptors.

Preliminary biological assay

A preliminary biological assay was performed in order to verify the binding ability of the cyclic CCK8 analogue towards the entire CCK_A receptor expressed in cultured cells. For these experiments the sulfated peptide derivative, cyclo^{29,34}[Tyr²⁷-(SO₃H),Dpr²⁹,Lys³⁴]-CCK8 (**2**) was used. In fact, the presence of the sulfate moiety on the Tyr²⁷ side chain should give an additional interaction with R197 of the CCK_A receptor. The R197 residue does not belong to residues 1–47 of the N-terminal end; this justifies the use of the nonsulfated peptide when the fragment CCK_A-R(1–47) is used as the receptor model and the use of the sulfated derivative for binding measurements to the entire receptor. The binding measurements were obtained by competition with the labelled linear peptide [¹¹¹In]DTPAGlu-Gly-[Tyr²⁷(SO₃H)]-CCK8 (DTPAGlu = *N,N*-bis[2-[bis(carboxyethyl)amino]ethyl]-L-glutamic acid), which displays a high affinity for the CCK_A receptor ($K_d \approx 10^{-9}$ M). The data obtained (Figure 8) show a typical pattern of competitive interaction with reduction in binding of the radiolabelled tracer at relatively high concentrations of the unlabelled cyclo^{29,34}[Tyr²⁷(SO₃H),Dpr²⁹,Lys³⁴]-CCK8. Fitting of the data yielded a 50% inhibitory concentration (IC₅₀) of 15 μ M.

Conclusion

The NMR structure of the complex between CCK8 and the CCK_A-R(1–47) receptor fragment reported by Pellegrini and Mierke^[6] allowed us to design a CCK8 analogue, cyclo^{29,34}[Dpr²⁹,Lys³⁴]-CCK8, whose backbone conformation is stabilised because of the cyclic skeleton. To the best of our knowledge, this is the first attempt to synthesise a cyclic agonist of CCK8 based on the structural knowledge of the bimolecular complex between the CCK_A receptor and its natural ligand. Binding of cyclo^{29,34}-[Dpr²⁹,Lys³⁴]-CCK8 to the receptor fragment CCK_A-R(1–47), measured by fluorescence quenching of the tryptophan residue, is characterised by a dissociation constant in the submicromolar range, not so far from that of the nonsulfated CCK8 ligand.^[12] The experimental structure of cyclo^{29,34}[Dpr²⁹,Lys³⁴]-CCK8 (obtained in DPC/water) confirms the presence of a turn-like conformation in the Trp³⁰–Met³¹ region, as predicted by the structure-based drug design. This structural motif enables the Trp³⁰ and Met³¹ side chains to adopt a suitable spatial orientation for interaction with the CCK_A receptor. The cyclic constraint between the Dpr²⁹ side chain and the CCK8 carboxyl terminus (Lys³⁴) introduces a restriction in the backbone conformational freedom, although the interaction with micelles still appears to be important to further stabilise the bioactive conformation. NMR structural data also indicate that the Lys³⁴ N ϵ amino group and the N-terminal

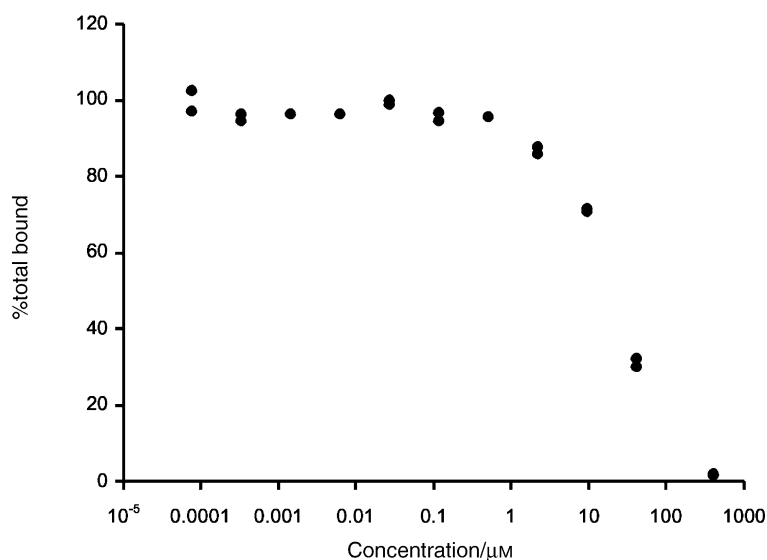


Figure 8. Competitive binding of cyclo^{29,34}[Tyr²⁷(SO₃H),Dpr²⁹,Lys³⁴]-CCK8 against [¹¹¹In]DTPAGlu-Gly-[Tyr²⁷(SO₃H)]-CCK8. The tracer is displaced by the cyclic derivative at high concentration with an apparent IC₅₀ value of approximately 15 μM (see the text for further details).

amino group extend towards a region that is expected not to be crucial for receptor binding. Both positions are therefore suitable for the introduction of a chelating agent to obtain metal-labelled derivatives. The structural characterisation of cyclo^{29,34}[Dpr²⁹,Lys³⁴]-CCK8 is an important starting point for the design of new cyclic analogues endowed with improved in vitro and in vivo binding to cells that overexpress the CCK_A receptors.

Experimental Section

Design: Energy minimisations were carried out with the program DISCOVER, version 2.98, implemented in the BIOSYM software package. Calculations were performed by using the consistent valence force field (CVFF)^[17–19] without cross- and Morse terms on a Silicon Graphics Octane workstation. The package INSIGHT/DISCOVER (Biosym Technologies, San Diego, CA), version 2000, was employed for model-building procedures, as a graphic interface, and for energy-minimisation procedures. The minimisation was carried out by using the conjugate gradient method until the energy difference between two subsequent steps was lower than 0.01 kJ mol⁻¹.

Peptide synthesis: The 47 residue peptide CCK_A-R(1–47) was synthesised in our laboratory as previously reported.^[12] DTPAGlu-Gly-[Tyr²⁷(SO₃H)]-CCK8 was purchased from INBIOS srl (Pozzuoli, Italy).

Cyclo^{29,34}[Dpr²⁹,Lys³⁴]-CCK8 (1), the cyclic peptide analogue of the natural ligand CCK8, was prepared by solid-phase methods, with standard Fmoc procedure on a fully automated Shimadzu SPPS-8 peptide synthesiser followed by peptide cyclisation and side-chain deprotection in solution.

The first amino acid residue, Fmoc-Lys(Boc)-OH (Boc = *tert*-butoxy-carbonyl), was coupled to 2-chlorotrityl chloride resin (0.82 mmol g⁻¹) under basic conditions (4 equiv DIPEA) in CH₂Cl₂. After removal of the Fmoc protecting group with 20% piperidine in *N,N*-dimethylformamide (DMF), the peptide chain was constructed by sequential coupling and deprotection of the following Fmoc-

protected amino acid derivatives: Fmoc-Phe-OH, Fmoc-Asp(OtBu)-OH, Fmoc-Met-OH, Fmoc-Trp(Boc)-OH, Fmoc-Dpr(Dde)-OH, Fmoc-Met-OH, Fmoc-Tyr(*t*Bu)-OH. The amino acid derivative for the final coupling was Boc-Asp(OtBu)-OH. All couplings were performed twice for 2 h, by using an excess of 4 equiv for the single amino acid. The α-amino acids were activated in situ by the standard pyBOP/1-hydroxy-1*H*-benzotriazole (HOBt)/DIPEA procedure. After completion of the synthesis the resin was treated twice for 10 min with 2% hydrazine in DMF in order to remove the Dde group from the Dpr residue β-NH₂ function. The deprotection procedure was shown to be complete by a ninhydrin test.

The linear peptide was cleaved from the solid support by suspending the resin in 1% CF₃COOH in CH₂Cl₂ with stirring for 1 min. The resin was then filtered and the filtrate was poured into 10% pyridine in CH₃OH. This procedure was repeated 10 times. After being filtered, the mixture was concentrated under reduced pressure and the crude product was isolated by precipitation into cold water. The precipitate was collected by centrifugation and dried in vacuo (over P₂O₅ pellets).

The protected peptide was then cyclised in CH₂Cl₂ by PyBOP/DIPEA activation with stirring for 5 h. After removal of the solvent under reduced pressure, the peptide was fully deprotected with CF₃COOH/H₂O/1,2-ethanedithiol (94:4:2) over 3 h. The solution was then concentrated and the crude product was isolated by precipitation into cold diethyl ether. The precipitate was collected by centrifugation and dried in vacuo (over KOH pellets).

Analytical RP-HPLC was carried out on a Shimadzu LC instrument equipped with SPDM AV-10 diode array and SIL-10A autosampler. A Phenomenex C₁₈ column (4.6 × 250 mm, 5 μm, 300 Å) was used, eluted with H₂O containing 0.1% trifluoroacetic acid (TFA; eluent A) and CH₃CN containing 0.1% TFA (eluent B) in a linear gradient from 20 to 80% of eluent B over 20 min at 1 mL min⁻¹ flow rate. Analysis of the crude product by analytical RP-HPLC showed a main peak at 16.6 min. Preparative RP-HPLC was carried out on a Waters Delta Prep 4000 instrument equipped with a UV lambda-Max model 481 detector and a Vydac C₁₈ column (22 × 250 mm, 15 μm, 300 Å) with the same eluents and gradient used for the analytical scale and at 20 mL min⁻¹ flow rate. The collected fractions containing the peptide were lyophilised and analysed: analytical HPLC showed a single peak at 16.6 min with a purity higher than 98%. The peptide identity was confirmed by mass spectral analysis carried out on MALDI-TOF Voyager-DE mass spectrometer (PerSeptive Biosystems), which gave a molecular ion peak [M – H]⁻ of 1202. The yield was 20%.

Cyclo^{29,34}[Tyr²⁷(SO₃H),Dpr²⁹,Lys³⁴]-CCK8 (2), the sulfated cyclic peptide derivative, was prepared by using the same standard solid-phase strategy as previously described for the cyclic CCK8 analogue 1. The tyrosine derivative Fmoc-Tyr(SO₃H) barium salt was used in order to achieve a peptide containing a sulfated tyrosine residue. After peptide cyclisation, in order to minimise the loss of the sulfate group during the final deprotection step, the protected and cyclic peptide was treated with the mixture CF₃COOH/H₂O/2-methylindole/*m*-cresole (87:10:2:1) for 16 h at +4 °C.^[10] The crude product was purified by preparative RP-HPLC and the purity assessed by analytical RP-HPLC. The system solvent used, both for analytical and preparative HPLC, was 0.1 M AcONH₄ in water (eluent A) and CH₃CN (eluent B) in a linear gradient from 5 to 95% of eluent B over 30 min. Analytical HPLC shows a single peak at 20.1 min with a purity higher than 98%. The peptide identity was confirmed by mass spectral

analysis, which gave a molecular ion peak $[M - H]^-$ of 1284. The yield was 13%.

NMR spectroscopy: DPC- d_{38} (98.96% isotopic enrichment) and 5-DS were purchased from CDN Isotopes Inc. (Pointe-Claire, Quebec) and Aldrich-Isotec, respectively, and were used without further purification. To obtain the structure of cyclo 29,34 [Dpr 29 ,Lys 34]-CCK8 in water solution, peptide (1.1 mg) was dissolved in deionised water (600 μ L) and D $_2$ O (40 μ L) was added (or the peptide was dissolved into 640 μ L of D $_2$ O), to obtain a final peptide concentration of 1.4 mM. The pH value was adjusted to 6.4 ± 0.1 by adding small amounts of NaOH. For experiments with DPC micelles, cyclo 29,34 [Dpr 29 ,Lys 34]-CCK8 (1.1 mg) was dissolved into a freshly prepared solution (640 μ L) containing 174 mM DPC- d_{38} in H $_2$ O/D $_2$ O 94%. The pH value was adjusted with diluted NaOH to 6.4 ± 0.1 . The final peptide concentration was 1.4 mM. The experiment with the spin label 5-DS in the presence of DPC micelles was carried out by adding solid 5-DS (610 μ g) to a solution (600 μ L) containing 1.4 mM cyclo 29,34 -[Dpr 29 ,Lys 34]-CCK8 and 174 mM DPC- d_{38} in H $_2$ O/D $_2$ O 94%, followed by readjusting the pH value to 6.4. The samples were transferred into 5-mm tubes for NMR analyses. NMR experiments were carried out on a Bruker Avance 600 spectrometer operating at 14 T (corresponding to a proton Larmor frequency of 600.13 MHz) and equipped with a triple-axis pulse field gradient (PFG) probe optimised for 1 H detection. Water suppression was achieved by means of the WATERGATE 3-9-19 pulse train^[20, 21] in the case of H $_2$ O/D $_2$ O 95% mixtures or by presaturation of the solvent line during the recycle delay for samples dissolved in D $_2$ O. Chemical shifts were referenced to external tetramethylsilane (0.03% in deuterated chloroform, coaxial insert). 2D-TOCSY (total correlation spectroscopy) experiments^[22] were carried out by means of a MLEV17 spin-lock pulse sequence^[23] flanked by two 2.5-ms trim-pulses with a spin-locking field strength of 10 KHz. The STATES time-proportional phase increment (TPPI) phase cycling scheme was used to obtain complex data points in the t_1 dimension. Typically, the following instrumental settings were used for TOCSY experiments: spectral width of 6900 Hz, 512 and 2048 complex data points in the t_1 and t_2 dimensions, respectively, 32–64 scans per t_1 increment, relaxation delay of 3 s, isotropic mixing time of 80–100 ms. The data were apodised with a square cosine window function and zero filled to a matrix of size 1024×1024 prior to FT and baseline correction. 2D-NOESY (nuclear Overhauser effect spectroscopy) experiments^[24] were carried out by the standard pulse sequence with the STATES TPPI phase cycling scheme with mixing times ranging from 100–450 ms. Typical instrumental settings included: spectral width of 6900 Hz in both f_1 and f_2 , 2048 \times 512 data points in t_2 and t_1 , respectively, 32–64 scans per t_1 increment, recycle delay of 3 s. The data were apodised along both t_1 and t_2 dimensions with a square cosine window function and zero filled to a symmetrical matrix of size 1024×1024 prior to FT and baseline correction. 2D-DQF-COSY (double quantum filtered correlation spectroscopy) experiments^[25] were obtained in the phase-sensitive mode by means of the TPPI method with the standard double quantum filtered pulse sequence coupled with a combination of PFG at the magic angle and selective water excitation to achieve optimal water suppression. Typical instrumental settings included: spectral width of 6600 Hz in f_1 and f_2 , 4096 \times 512 data points in t_2 and t_1 , respectively, recycle delay of 3 s, 64 scans per t_1 increment. The data were apodised with a square cosine window function and zero filled to a matrix of size 2048×2048 prior to FT and baseline correction.

Molecular dynamics: All calculations were carried out on a Silicon Graphics Octane workstation. The assignment of 1 H NMR signals and integration of NOE peaks were done by means of the XEASY^[26] software package. The assignment of 1 H NMR resonances was carried

out by the sequence-specific method,^[27] that is, by iterative comparison of the TOCSY, NOESY and DQF-COSY spectra. A number of ambiguities in the assignment due to severe signal overlap could be resolved by comparing experiments carried out at different temperatures (285–310 K). The structure optimisation based on NMR constraints was carried out by the DYANA^[28] program (energy minimisation by torsion angle dynamics and simulated annealing) and the structure analysis was performed by means of the MOLMOL^[29] program (molecular graphics). Peak volumes were obtained from NOESY spectra acquired with mixing times of 450 ms (aqueous solution) and 150 ms (DPC micelles). Upper distance limits involving diastereotopic atom pairs without stereospecific assignment were increased in order to allow for both assignments as described in ref. [30]. To account for the effect of local motions on the intensity of the NOE signals, the peak volume to internuclear upper limit bound conversion was executed by classifying the NOE interactions into three different calibration classes and applying to each of them a different calibration function, following the DYANA standard procedure. Typically, 800–1000 conformers with random values of both backbone and side-chain dihedral angles were generated (bond length and bond angles were fixed at their optimal values according to the ECEPP/2^[31] standard geometry). DYANA minimisations were carried out with 5000 TAD steps and the contribution to the target function due to the violation of the upper limit distance constraints was calculated according to a square potential function. The optimised conformers were accepted if their residual target function was below the cut-off value of 0.18 \AA^2 and if they did not present any consistent steric or geometric violation. A subgroup of structures endowed with lowest target function values was extracted from the ensemble of acceptable ones for further structural analyses. Typically, a subgroup of 30 structures represented a good compromise between sufficient statistics and data manageability for analysis and computer graphics. These structures were forwarded to the MACROMODEL 6.5 software package (Columbia University, NY)^[11] for further molecular dynamics minimisations with the AMBER* forcefield.^[32, 33] Typically, 10–50 ps of restrained MD at 300 K were carried out for structure refinement. Experimental constraints were introduced with a force constant of $100 \text{ kJ mol}^{-1} \text{\AA}^{-2}$. For final energy minimisation, the structures were subjected to 500 iteration molecular mechanics cycles with the Polak–Ribiere conjugate gradient minimisation mode. The value of the derivative convergence criterion was $0.5 \text{ kJ mol}^{-1} \text{\AA}^{-1}$. Energy minimisations were performed in vacuo.

Absorption spectroscopy: All concentrations were measured on a Jasco Model V-550 spectrophotometer. Absorptivities (ϵ_{280}) used were 5630 and $6845 \text{ m}^{-1} \text{cm}^{-1}$ for CCK $_A$ -R(1–47) and cyclo 29,34 -[Dpr 29 ,Lys 34]-CCK8, respectively. These values were calculated by adding individual contributions from tyrosyl and tryptophanyl residues present in the primary structures^[34] (1215 and $5630 \text{ m}^{-1} \text{cm}^{-1}$, respectively^[35]). It was estimated that this procedure is affected by a maximum error of 5%.^[36] Before measurements, all solutions were centrifuged and filtered and their limpidity was checked by absorbance at 325 nm, where absorption should be negligible.

Fluorescence measurements: The interaction between CCK $_A$ -R(1–47) and cyclo 29,34 [Dpr 29 ,Lys 34]-CCK8 was monitored at room temperature by selectively exciting tryptophan fluorescence at 295 nm on a Jasco Model FP-750 spectrofluorimeter. Emission spectra were recorded by using equal excitation and emission bandwidths, a recording speed of 125 nm min^{-1} and automatic selection of the time constant. Binding curves were obtained according to the limiting reagent method. Namely, several small volumes of concentrated cyclo 29,34 [Dpr 29 ,Lys 34]-CCK8 dissolved in 10 mM phosphate solution

(pH 7.2) were added a fixed volume of CCK_A-R(1–47) dissolved in the same buffer in the presence of 6–8 mM SDS to mimic a membrane environment.^[37] In all cases, the total absorbance of the solutions was less than 0.1 at the excitation wavelength, which ensured fluorescence linearity. After each addition, the reaction mixture was left to stand until an apparent equilibrium was reached, as judged by the constancy of the fluorescence signal. Final spectra were always obtained after blank correction, adjustment for dilution and subtraction of the separate contributions of cyclo^{29,34}[Dpr²⁹,Lys³⁴]-CCK8 and CCK_A-R(1–47) from the total fluorescence. This allowed us to detect fluorescence modifications produced by the binding interaction, which were thereafter used to calculate the K_d value between the interacting species.

Treatment of binding data: Fluorescence intensities at 335 nm, obtained as stated above, were used to evaluate the bound fraction of CCK_A-R(1–47), α , by using Equation (1), where F is the observed fluorescence at 335 nm and F_0 and F_∞ refer to the fluorescence of free and bound CCK_A-R(1–47), respectively.

$$\alpha = (F - F_0)/(F_\infty - F_0) \quad (1)$$

Subsequent fitting to Equation (2), implemented in the program Scientist for Windows, version 2.0 (MicroMath Software, San Diego, CA), allowed us to evaluate K_d . Here, P_0 and L_0 stand for the total concentrations of CCK_A-R(1–47) and cyclo^{29,34}[Dpr²⁹,Lys³⁴]-CCK8, respectively.

$$\alpha = \{K_d + P_0 + L_0 - [(K_d + P_0 + L_0)^2 - 4P_0L_0]^{1/2}/(2P_0) \quad (2)$$

Equation (2) holds for one-site binding equilibria and can be easily derived from Equation (3) by considering that the molar concentration of free cyclo^{29,34}[Dpr²⁹,Lys³⁴]-CCK8, $[L]$, equals $L_0 - \alpha P_0$.

$$(F - F_0)/(F_\infty - F_0) = [L]/(K_d + [L]) \quad (3)$$

Concerning the K_d fitting procedure, F_0 was always fixed to zero, which represents the fluorescence change before any ligand addition, P_0 was set equal to its actual value (0.49–2.40 μ M), as determined by absorbance at 280 nm and F_∞ was measured after saturation of the receptor binding sites with as large a molar excess of cyclo^{29,34}[Dpr²⁹,Lys³⁴]-CCK8 as possible. After data smoothing by the Savitzky–Golay filter, implemented in the mathematical package used, preliminary convergence was accomplished by means of several steps of simplex optimisation. Then, final values of K_d were obtained by the Levenberg–Marquardt minimiser and averaged out. In some experiments, F_∞ values were hard to assess owing to saturation of the fluorescence signal on addition of large amounts of cyclo^{29,34}[Dpr²⁹,Lys³⁴]-CCK8. This hampered the achievement of very high ligand:receptor ratios. In such cases, both F_∞ and K_d were chosen as fitting parameters.

Preliminary biological assay: Competition binding experiments were performed on A431 cells that had been stably transfected with the pRFE-neoplasmid containing the full coding sequence for the human CCK_A receptor.^[38] DTPA-Glu-Gly-[Tyr²⁷(SO₃H)]-CCK8 was labelled with ¹¹¹In as described for unsulfated DTPA-Glu-Gly-CCK8.^[39] Fixed tracer amounts of the labelled peptide were incubated with the receptor-expressing cells in the presence of cyclo^{29,34}[Tyr²⁷(SO₃H),Dpr²⁹,Lys³⁴]-CCK8 at concentrations ranging from 10⁻¹⁰–10⁻³ M. The amount of bound radioactivity was determined after 1 h at 4 °C. Nonlinear regression analysis with a model for homologous competition binding was performed by using the

GraphPad Prism program (version 3.0a for Macintosh; GraphPad Software, San Diego, CA; www.graphpad.com.) to derive the 50% inhibitory concentration (IC₅₀).

Supporting Information: Supporting Information is available listing all the upper limit distances used to obtain the structural models of cyclo^{29,34}[Dpr²⁹,Lys³⁴]-CCK8 in aqueous solution and in DPC/water (Tables S1 and S2).

Acknowledgements

This work was supported by grants from Italian MIUR (Ministry of Education, University and Research) (Progetto Oncologia), and from Bracco Imaging spa, Milan, Italy. We are grateful to Dr. Daniel Fourmy (Institut Louis Bugnard, Toulouse, France) for generously providing the pRFE-neo-CCKAR plasmid.

Keywords: binding studies · CCK analogues · conformation analysis · cyclic peptides · ligand design

- [1] J. F. Rehfeld, W. W. Van Soulinge, *Adv. Cancer. Res.* **1994**, *63*, 295–347.
- [2] R. J. Deschenes, L. J. Lorenz, R. S. Haun, B. A. Roos, K. J. Collier, J. E. Dixon, *Proc. Natl. Acad. Sci. USA* **1984**, *81*, 726–730.
- [3] S. A. Wank, *Amer. J. Physiol.* **1995**, *269*, G628–G646.
- [4] P. de Tullio, J. Delarge, B. Piroette, *Curr. Med. Chem.* **1999**, *6*, 433–455.
- [5] A. Escherich, J. Lutz, C. Escrieut, D. Fourmy, A. S. van Neuren, G. Mueller, A. Schafferhans, G. Klebe, L. Moroder, *Biopolymers* **2001**, *56*, 55–76.
- [6] M. Pellegrini, D. F. Mierke, *Biochemistry* **1999**, *38*, 14775–14783.
- [7] C. Giragossian, D. F. Mierke, *Biochemistry* **2001**, *40*, 3804–3809.
- [8] J. D. Garner, M. D. Walker, J. Martinez, G. P. Priestly, S. Natarayan, M. Bodanszky, *Biochim. Biophys. Acta* **1980**, *630*, 323–329.
- [9] V. Giglioux, B. Maigret, C. Escrieut, S. Silvente-Poirot, M. Bouisson, J. Fehrentz, L. Moroder, D. Gully, J. Martinez, N. Vaysse, D. Fourmy, *Protein Sci.* **1999**, *8*, 2347–2354.
- [10] K. Kitagawa, C. Aida, H. Fujiwara, T. Tagami, S. Futaki, M. Kogire, J. Ida, K. Inoue, *J. Org. Chem.* **2001**, *66*, 1–10.
- [11] F. Mohamadi, N. G. J. Richards, W. C. Guida, R. Liskamp, M. Lipton, C. Caufield, G. Chang, T. Hendrickson, W. C. Still, *J. Comput. Chem.* **1990**, *11*, 440–467.
- [12] R. Ragone, S. De Luca, D. Tesaro, C. Pedone, G. Morelli, *Biopolymers* **2001**, *56*, 47–53.
- [13] E. De Vendittis, G. Palumbo, G. Parlato, V. Bocchini, *Anal. Biochem.* **1981**, *115*, 278–286.
- [14] C. Esposito, P. Colicchio, A. Facchiano, R. Ragone, *J. Colloid Interface Sci.* **1998**, *200*, 310–312.
- [15] B. Charpentier, A. Dor, P. Roy, P. England, H. Pham, C. Durieux, B. P. Roques, *J. Med. Chem.* **1989**, *32*, 1184–1190.
- [16] F. Noble, B. P. Roques, *Prog. Neurobiol.* **1999**, *58*, 349–379.
- [17] S. Lifson, A. T. Hagler, P. J. Dauber, *J. Am. Chem. Soc.* **1979**, *101*, 5111–5121.
- [18] A. T. Hagler, S. Lifson, P. J. Dauber, *J. Am. Chem. Soc.* **1979**, *101*, 5122–5130.
- [19] A. T. Hagler, P. J. Dauber, S. Lifson, *J. Am. Chem. Soc.* **1979**, *101*, 5131–5140.
- [20] M. Piatto, V. Saudek, V. Sklenar, *J. Biomol. NMR* **1992**, *2*, 661–666.
- [21] V. Sklenar, M. Piatto, R. Leppik, V. Saudek, *J. Magn. Reson.* **1993**, *A102*, 241–245.
- [22] L. Braunschweiler, R. R. Ernst, *J. Magn. Reson.* **1983**, *53*, 521–528.
- [23] A. Bax, D. G. Davis, *J. Magn. Reson.* **1985**, *65*, 355–360.
- [24] J. Jeener, B. H. Meier, P. Bachmann, R. R. Ernst, *J. Chem. Phys.* **1979**, *71*, 4546–4553.
- [25] U. Piantini, O. W. Sørensen, R. R. Ernst, *J. Am. Chem. Soc.* **1982**, *104*, 6800–6801.
- [26] C. H. Bartels, T.-H. Xia, M. Billeter, P. Güntert, K. Wüthrich, *J. Biomol. NMR* **1995**, *6*, 1–10.

- [27] K. Wüthrich, *NMR of proteins and nucleic acids*, John Wiley and Sons, New York, **1986**.
- [28] P. Güntert, C. Mumenthaler, K. Wüthrich, *J. Mol. Biol.* **1997**, *273*, 283–298.
- [29] R. Koradi, M. Billeter, K. Wüthrich, *J. Mol. Graphics* **1996**, *14*, 51–55.
- [30] P. Güntert, *Quart. Rev. Biophys.* **1998**, *31*, 145–237.
- [31] G. Némethy, M. S. Pottle, H. A. Scheraga, *J. Phys. Chem.* **1983**, *87*, 1883–1887.
- [32] S. J. Weiner, P. A. Kollman, D. A. Case, U. C. Singh, C. Chio, G. Alagona, S. Profeta, P. Weiner, *J. Am. Chem. Soc.* **1984**, *106*, 765–784.
- [33] D. Q. McDonald, W. C. Still, *Tetrahedron Lett.* **1992**, *33*, 7743–7746.
- [34] H. Edelhoch, *Biochemistry* **1967**, *6*, 1948–1954.
- [35] C. N. Pace, F. Vajdos, L. Fee, G. Grimsley, T. Gray, *Protein Sci.* **1995**, *4*, 2411–2423.
- [36] S. C. Gill, P. H. von Hippel, *Anal. Biochem.* **1989**, *182*, 319–326.
- [37] M. R. Eftink, *Methods Enzymol.* **1997**, *278*, 221–257.
- [38] K. Kennedy, C. Escrieut, M. Dufresne, P. Clerc, N. Vaysse, D. Fourmy, *Biochem. Biophys. Res. Commun.* **1995**, *213*, 845–852.
- [39] L. Aloj, M. R. Panico, C. Caraco, A. Zannetti, S. Del Vecchio, C. Di Nuzzo, C. Arra, G. Morelli, D. Tesaro, S. De Luca, C. Pedone, M. Salvatore, *Biopolymers* **2003**, *66*, 370–380.

Received: April 24, 2003 [F 635]